Elastomeric microfluidic diode and rectifier work with Newtonian fluids

John Liu,[1] Yan Chen,[2] Clive R. Taylor,[3] Axel Scherer,[2] and Emil P. Kartalov[2,3,a]

[1]*Department of Applied Physics, California Institute of Technology, Pasadena, California 91125, USA*
[2]*Department of Electrical Engineering, California Institute of Technology, Pasadena, California 91125, USA*
[3]*Department of Pathology, University of Southern California, Los Angeles, California 90089-9092, USA*

We report on two microfluidic elastomeric autoregulatory devices—a diode and a rectifier. They exhibit physically interesting and complex nonlinear behaviors (saturation, bias-dependent resistance, and rectification) with a Newtonian fluid. Due to their autoregulatory properties, they operate without active external control. As a result, they enable increased microfluidic device density and overall system miniaturization. The demonstrated diode and rectifier would also be useful components in future microfluidic logic circuitry. © *2009 American Institute of Physics.* [doi:10.1063/1.3268463]

I. INTRODUCTION

One of the wonderful applications of microfluidics is the study of complex fluidic phenomena at low Reynolds numbers. Accordingly, scientifically interesting nonlinear devices and techniques have emerged in recent years. For example, the curious properties of a non-Newtonian fluid have been utilized to demonstrate anisotropic resistance in one-layer microfluidic chips.[1] Bubble-logic devices[2] have exhibited nonlinearity, bistability, gain, synchronization, cascading, feedback, and programmability, thereby laying down much groundwork for future fluidic logic. One- and two-input microfluidic gates[3] have been demonstrated using actuation by controlling flow resistance. A flap-based microfluidic diode[4] and valves[5–9] constricting flow in one direction have been built.

However, various aspects of the above devices make it challenging to build and use them in inexpensive gas-permeable materials,[10–12] which are thought best for biological applications.[13] Some devices require exotic working fluids, some use two-phase systems carrying risks,[13] some need active external control, and some are simply too difficult to fabricate and/or operate to a consistently high quality.

By contrast, herein we present autoregulatory devices (diode and rectifier), which are reliable and easy to fabricate. The devices function based on an established autoregulatory technique utilizing detour channels.[14,15] They work with plain water, exhibit complex nonlinear behavior, and operate without active external control.

Active control poses a serious problem for further integration and miniaturization.[14–16] Pressure inputs take up significant "real estate" on the chip and have to be individually connected, making the devices relatively big and awkward to use. Also, each independent line of external control requires its own macroscale pressure transducer (typically a solenoid Lee valve[17]), increasing overall system size and cost. Hence, while a few applications[18,19] of high inherent parallelism

lend themselves to disproportionately simple control structure, the architectural and operational price of active control remains a principal source of practical limitations in the field. Consequently, as autoregulators exhibit complex fluidic behavior without active external control, they offer a path toward increased sophistication, greater device density, and enhanced miniaturization in the field.

II. MATERIALS AND METHODS

A. Mold fabrication

The thick-layer mold and low features on the thin-layer mold. The wafer was exposed to hexamethyldisilazane vapor for 3 min. SPR220-7 was spun at 1000 rpm for 60 s. The wafer was baked for 2 min at 105 °C, exposed to UV for 1.75 min, developed in 100% 319 developer for 1 min, rinsed in water, blown dry, and hard baked for 10 min at 140 °C with a 5 min ramp up and ramp down.

The high features on the thin-layer mold. Su8-2025 was spun at 1500 rpm for 60 s. The wafer was baked for 5 min at 65 °C and 10 min at 95 °C, exposed to UV for 6 min, baked again for 2 min at 65 °C and 6 min at 95 °C, developed in 100% Su8 developer for 2 min, rinsed in fresh developer, blown dry, and hard baked for 10 min at 150 °C with a 5 min ramp up and ramp down.

B. Chip fabrication

Dow Corning Sylgard 184 polydimethylsiloxane (PDMS) monomer (20 g) and cross-linker (1 g) were mixed for the thin layer. Separately, monomer (35 g) and cross-linker (7 g) were mixed for the thick layer. The mixtures were stirred (1 min) and degassed (2 min) in a HM-501 hybrid mixer (Keyence, Long Beach, CA). Molds were exposed to trimethylchlorosilane vapors for 3 min. The thin layer was spun at 2500 rpm for 60 s in a P6700 spincoater (Specialty Coating Systems, Indianapolis, IN). The layers were baked for 25 min at 80 °C. The thick layer was released from the mold, diced, perforated to form ports, cleaned with ethanol, blown dry, and aligned and assembled onto the thin layer. The assembly was baked for 55 min at

a)Author to whom the correspondence should be addressed. Electronic mail: kartalov@usc.edu. Tel.: (323) 442-3211.

106, 114311-1

80 °C, diced, released from the mold, perforated to form ports, cleaned with ethanol, blown dry, and assembled to a clean glass slide. The resulting chips were baked for 8 h at 80 °C. The same protocol was used in both the diode and rectifier projects.

C. Device parameters

Diode: Varying the X/L ratio. The valves were 100×150 μm^2 $(L \times W)$, the lower channels were 7×100 μm^2 $(H \times W)$, and the upper channels were 25×100 μm^2 $(H \times W)$. The length of the main channels was $L = 14.2$ mm.

Diode: Varying the push-up valve width. The valve widths ranged from 100 to 330 μm, the lower channels were 12×100 μm^2 $(H \times W)$, and the upper channels were 14×100 μm^2 $(H \times W)$. The length of the main channels was $L = 14.2$ mm and $(X_1/L, X_2/L)$ was set at (0.66, 0.15).

Rectifier. The valves were 100×140 μm^2 $(L \times W)$, the lower channels were 15.5×100 μm^2, and the upper channels were 14×100 μm^2 $(H \times W)$. The length of the main channels was $L = 10.1$ mm and X/L was set at 0.77.

D. Experimental setup

The microfluidic fluorescence microscopy station contains an inverted Olympus IX-71 fluorescence microscope (Olympus America, Melville, NY) equipped with a mercury lamp (HBO® 103 W/2; OSRAM Munich, Germany) and a cooled charge-coupled device camera ST-7I (Santa Barbara Instrument Group, Santa Barbara, CA). 23-gauge steel tubes (New England Small Tube, Litchfield, NH) are inserted into the ports of the chip and connected through Tygon® tubing (Cole-Parmer, Vernon Hills, IL) to a pressure source, controlled by AirTrol regulators, and measured by a digital gauge from TIF Instruments.

E. Experimental procedure

Diodes. Air was removed from the device by closing a shutoff valve at the exhaust and forcing water in under pressure. The trapped air escaped through the gas-permeable PDMS matrix. Then the shutoff valve was opened and throughput was measured by timing the advance of the water meniscus in transparent tubing connected to the exhaust.

Rectifiers. Air was removed from the device by closing shutoff valves in the top right and bottom left corners of the device and forcing water in under pressure. The trapped air escaped through the gas-permeable PDMS matrix. Then the shutoff valves were opened and regular flow was established. The velocities of the beads were measured by dividing the lengths of the beads' trajectories by the respective camera exposure times in a series of fluorescence images. The fluid flow velocity at each pressure setting was obtained as the upper bound on the measured bead velocities.

III. RESULTS AND DISCUSSION

The morphological basis for autoregulation was established by microfluidic vias[14] (vertical passages), which enabled the construction of three-dimensional (3D) channels[14]
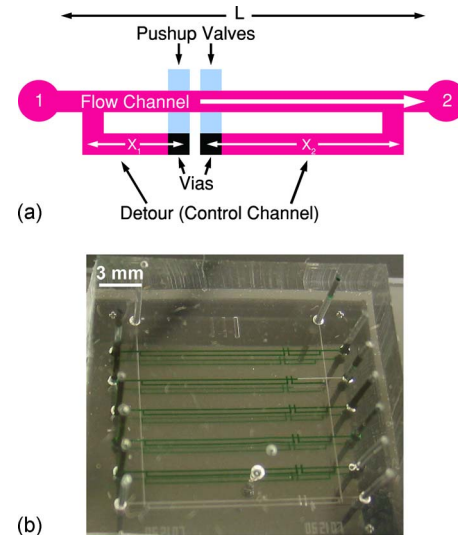

FIG. 1. (Color online) (a) An architectural diagram of the microfluidic diode. (b) Photo of a chip with diode devices. Microfluidic channels are filled with a green dye to make them stand out.

in multilayer microfluidic chips[17] built using soft lithography techniques.[20] Since microfluidic valves consist of a membrane between channels in different layers,[13,17] 3D channels were built to act upon themselves, creating nonlinear behavior and thus enabling autoregulation. A microfluidic current source[14] was demonstrated as the first device of this type.

We have arranged two such current sources back-to-back to produce a microfluidic diode [Fig. 1(a)]. Each constituent current source is a two-layer device where flow is established along a main channel (input to exhaust) in the upper layer (red). A detour channel splits from the main channel close to the input and continues through a via (black) into the lower layer (blue) to connect to a pushup valve,[21] which acts upon the main channel close to the exhaust. Static pressure decreases from input to exhaust as fluid flows along the main channel. Meanwhile, static pressure remains constant along the dead-end detour channel because there is no fluid flow along it. Therefore, the pushup valve at the end of the detour channel experiences an effective pressure equal to the static pressure drop between the channel split and the main-channel segment above the valve. Because of the device geometry and Poiseuille's law, as the applied pressure increases, the pressure drop also increases and the pushup valve membrane[21] deforms upward constricting the main channel. Hence, the total resistance increases with applied pressure, and the device behaves nonlinearly with Newtonian fluids. The current source saturates in forward bias and behaves linearly in reverse bias.

In the diode (Fig. 1), two current sources are arranged back to back. Hence, in each bias, one of the current sources will saturate while the other will remain linear. Thus the overall device should saturate in both biases. For a given main-channel length L, the detour ratios X_1/L and X_2/L can be chosen such that there will be a significant difference between the saturation levels of the two biases, resulting in a device that should be far more conductive in one flow direc-
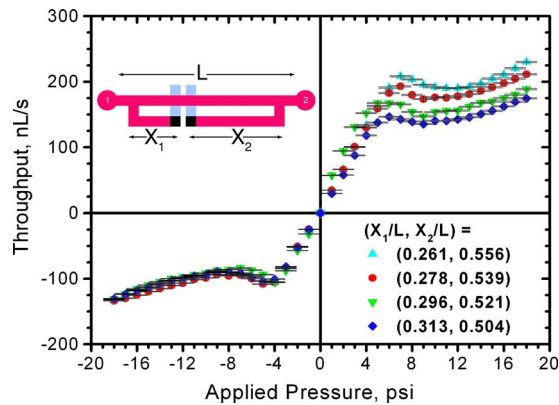
FIG. 2. (Color online) Throughput of the main flow channel vs applied pressure for different detour ratios (X/L). In the forward bias (positive pressure), the first (left) current source of detour length X_1 saturates. In the reverse bias (negative pressure), the second (right) current source of detour length X_2 saturates. Larger detour ratios (X/L) produce lower saturation levels.

FIG. 4. (Color online) A photo of the microfluidic rectifier device. Microfluidic channels are filled with green dye to make them stand out. The red arrow shows the direction of fluid flow in the central channel, which is the rectified output of the flow input applied between ports 1 and 2.

tion than in the other. Thus, while the analogy with electronics is not perfect, the overall device should behave as the fluidic equivalent of a diode.

A set of diodes was constructed in the same chip [e.g., Fig. 1(b)], wherein the valves' widths were kept constant at 150 μm, while the detour ratios ($X_1/L, X_2/L$) were varied. The devices were characterized by measuring their throughputs as a function of applied pressure. As predicted, larger detour ratios produce lower saturation levels (Fig. 2). Thus the detour ratios can be used to tune the saturation points of a diode as desired for any particular application. These results constitute experimental proof of principle for this type of microfluidic diode.

An autoregulator relies on a valve's constriction for its operation. On the other hand, the valve's behavior is determined by the valve's physical parameters.[22] Hence, it is reasonable to expect that varying those parameters would tune the behavior of the autoregulator as well.

To test this conjecture, we built a set of diodes on the same chip, where the detour ratios ($X_1/L, X_2/L$) were kept constant at (0.66, 0.15), while the valve widths ranged from 100 to 330 μm. The results (Fig. 3) show that the saturation
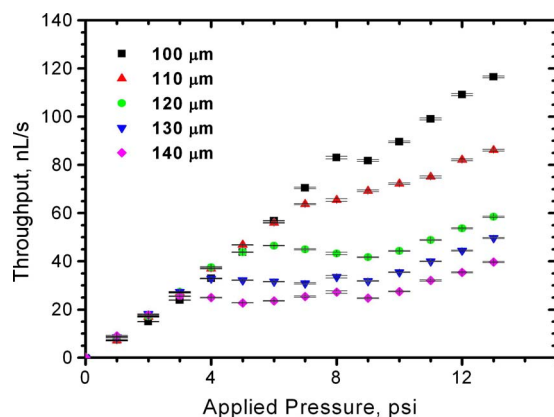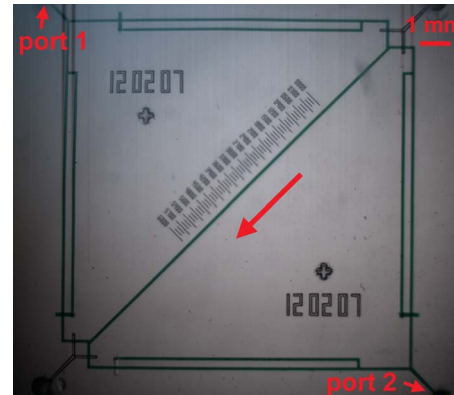

FIG. 3. (Color online) Throughput of the main flow channel vs applied pressure for pushup valve widths ranging from 100 μm (square) to 140 μm (diamond). The saturation pressure and throughput of each diode decrease as the pushup valve width increases.

pressure and throughput of the device decrease as the pushup valve width increases. Thus the valve parameters can be used to tune the saturation points of a diode.

The experiments also showed that with the chosen geometries and fabrication techniques, it is not practical to use valves, whose widths exceed 150 μm, because they would irreversibly stick shut either during fabrication or operation. This limitation may be circumvented by the construction of a series of valves connected to the same detour channel and acting upon the same main channel. Then, the overall resistance should increase roughly linearly with the number of valves, further lowering the saturation pressure and throughput of the overall device.

As pressure increases beyond the linear regime of the device, a slight dip in the T-P curve is consistently observed (Figs. 2 and 3). This effect may give new insights into the specific mechanics of valve deformation and channel constriction, since current valve models[22] focus only on valves in the fully closed state. Furthermore, utilization of this "negative resistance" phenomenon[23] may be useful in the pursuit of oscillatory behavior in autoregulatory architectures.

Following the analogy with electronics, we next designed a microfluidic rectifier by arranging four microfluidic diodes in the traditional rectifier bridge pattern. Taking a second look at the diagram, we realized that since each branch needs to saturate in only one bias, the diodes could be replaced with current sources, simplifying the overall device.

The resulting rectifier is shown in Fig. 4. If pressure is applied at port 1, the left and right current sources will be forward biased and thus should saturate, while the top and bottom ones will be reverse biased and thus should act as simple channels. Most of the fluid should therefore travel along a Z-shaped least-resistance pathway: through the top current source, the central channel, and the bottom current source. Similarly, if pressure is applied at port 2, the top and bottom current sources should saturate, while the left and right should act as simple channels. Hence, the pathway of least resistance should be through the right current source, the central channel, and then the left current source. Thus,
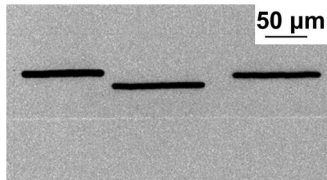
FIG. 5. A fluorescent bead's velocity is determined by measuring the length of the bead's trajectory in the fluorescence image for a set value of the photoexposure time. In this image, darker color corresponds to higher fluorescence intensity.

the fluid flow direction should remain the same in the central channel regardless of the pressure bias of the overall device.

To test this prediction, we had to measure the flow velocity inside the central channel over a range of pressures. To do so, we introduced fluorescent microspheres (beads) in the flow and tracked their progress by taking fluorescence images (e.g., Fig. 5). The length of the observed streaks was divided by the photoexposure time to produce a value for the velocity of the beads carried by the current. As a significant number of beads were imaged at each pressure setting, the fluid flow velocity could be estimated as the upper bound on the observed bead velocities at the channel's centerline. Figure 6 shows the experimental results: for any polarity of high input pressure, this device produced the same output polarity. These results offer a proof of principle for this type of microfluidic rectifier.

The specific shape of the curve can be explained as follows. At low pressures, forward-biased sources are unsaturated, and thus the entire system acts as simple channels. Then, symmetry of the design dictates that the pressures on both ends of the central channel are nearly equal. Hence the pressure difference is nearly zero, leading to nearly zero throughput and producing the observed flat section of the V-P curve close to the origin in both biases (Fig. 6). All operational devices produced this U shape for the T-P curve.

The device of Fig. 6 also shows another, far smaller effect; namely, the velocity dips slightly in the negative be-

fore the current sources reach saturation. This effect was observed to occur with other devices as well, at low pressure applied in either positive or negative direction. We attribute the effect to slight asymmetry in the linear resistances of the constituent channels, e.g., due to fabrication artifacts. It is important to note, however, that once the current sources reach saturation, the main rectification effect completely dominates such fabrication irregularities.

The recently reported lateral architecture[15] for detour autoregulation is single layer and thus easier to fabricate than our vertical architectures.[14] However, its required channel heights[15] (100 μm) confine its applicability to the thick topmost layer of conventional multilayer chips.[13] By contrast, our devices work with far smaller channels ($7-25$ μm tall), which makes them more compatible and integrable with the rest of the multilayer microfluidic technology and its numerous applications.[13]

The demonstrated diode and rectifier show promise for future use in microfluidic logic. Unlike other efforts[3] to achieve fluidic logic in single-phase Newtonian fluids, all the components of our devices operate in the same fluid. This feature ensures that input and output representations are identical, which leads to the possibility of cascaded architectures and fluidic computation.[24]

As the complexity of microfluidic design increases, the practical issue of economizing chip space and decreasing external control will become increasingly important. Hardwired during fabrication and requiring no active external control to operate, the presented devices can be of great utility in building the highly integrated complex microfluidic circuitry of the future.

IV. CONCLUSIONS

A microfluidic diode and rectifier have been built and proven to work with Newtonian fluids in elastomeric microfluidic devices. The saturation point of the diode can be tuned by varying the detour ratios and valve dimensions of the constituent current sources. The demonstrated devices are interesting from the fundamental perspective of the underlying physical behavior and from the practical perspective of reducing active external control. The latter is of particular importance in enhancing microfluidic miniaturization and facilitating practical applications. The demonstrated devices may also form useful components in future fluidic logic circuitry.
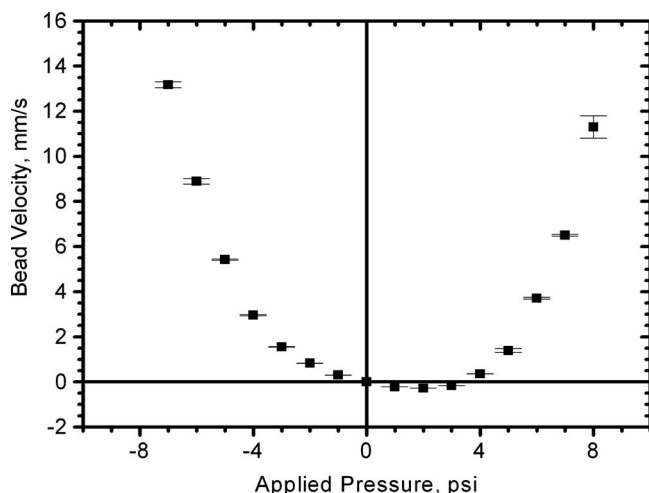
FIG. 6. Maximal bead velocity in the rectifier's central channel vs pressure applied between input ports 1 and 2. The device outputs the same polarity of throughput for both polarities of high input pressure, thus experimentally confirming rectification.

[1] A. Groisman and S. R. Quake, Phys. Rev. Lett. **92**, 094501 (2004).
[2] M. Prakash and N. Gershenfeld, Science **315**, 832 (2007).
[3] T. Vestad, D. W. Marr, and T. Munakata, Appl. Phys. Lett. **84**, 5074

(2004).

[4]M. L. Adams, M. L. Johnston, A. Scherer, and S. R. Quake, J. Micromech. Microeng. **15**, 1517 (2005).

[5]V. Seidemann, S. Butefisch, and S. Buttgenbach, Sens. Actuators, A **97-98**, 457 (2002).

[6]V. Seidemann, J. Rabe, M. Feldmann, and S. Büttgenbach, Microsyst. Technol. **8**, 348 (2002).

[7]E. F. Hasselbrink, Jr., T. J. Shepodd, and J. E. Rehm, Anal. Chem. **74**, 4913 (2002).

[8]W. Y. Sim, H. J. Yoon, O. C. Jeong, and S. S. Yang, J. Micromech. Microeng. **13**, 286 (2003).

[9]K. Hosokawa and R. Maeda, J. Micromech. Microeng. **10**, 415 (2000).

[10]T. C. Merkel, J. Polym. Sci., Part B: Polym. Phys. **38**, 3 (2000).

[11]C. M. Pusch, I. Wundrack, R. Müllenbach, W. Schempp, and N. Blin, Electrophoresis **23**, 20 (2002).

[12]R. Gómez-Sjöberg A. A. Leyrat, D. M. Pirone, C. S. Chen, and S. R. Quake, Anal. Chem. **79**, 8557 (2007).

[13]E. P. Kartalov, A. Scherer, W. F. Anderson, and J. Nanosci, Nanotechnology **6**, 2265 (2006).

[14]E. P. Kartalov, C. Walker, C. R. Taylor, W. French Anderson, and A. Scherer, Proc. Natl. Acad. Sci. U.S.A. **103**, 12280 (2006).

[15]I. Doh and Y. H. Cho, Lab Chip **9**, 2070 (2009).

[16]K. A. Shaikh, K. S. Ryu, E. D. Goluch, J.-M. Nam, J. Liu, C. S. Thaxton, T. N. Chiesl, A. E. Barron, Y. Lu, C. A. Mirkin, and C. Liu, Proc. Natl. Acad. Sci. U.S.A. **102**, 9745 (2005).

[17]M. A. Unger, H. P. Chou, T. Thorsen, A. Scherer, and S. R. Quake, Science **288**, 113 (2000).

[18]L. Hansen, E. Skordalakes, J. M. Berger, and S. R. Quake, Proc. Natl. Acad. Sci. U.S.A. **99**, 26 (2002).

[19]T. Thorsen, S. J. Maerkl, and S. R. Quake, Science **298**, 580 (2002).

[20]C. Duffy, J. C. McDonald, O. J. A. Schueller, and G. M. Whitesides, Anal. Chem. **70**, 4974 (1998).

[21]V. Studer, G. Hang, A. Pandolfi, M. Ortiz, W. French Anderson, and S. R. Quake, J. Appl. Phys. **95**, 393 (2004).

[22]P. Kartalov, A. Scherer, S. R. Quake, C. R. Taylor, and W. French Anderson, J. Appl. Phys. **101**, 064505 (2007).

[23]J. B. Gunn, Solid State Commun. **1**, 88 (1963).

[24]N. H. E. Weste and D. Harris, *CMOS VLSI Design* (Pearson Education, Boston, 2005).